Physics Letters A 375 (2011) 3483–3489

Contents lists available at ScienceDirect

Physics Letters A

www.elsevier.com/locate/pla

Thermal conductivity in a rigidity transition

Gerardo G. Naumis *, F. Salazar

Departamento de Física-Química, Instituto de Física, Universidad Nacional Autónoma de México (UNAM), Apartado Postal 20-364, 01000 México, Distrito Federal, Mexico

ARTICLE INFO

Article history:
Received 29 April 2011
Received in revised form 27 July 2011
Accepted 3 August 2011
Available online 9 August 2011
Communicated by A.R. Bishop

ABSTRACT

The thermal conductivity ($\kappa(T)$) in a lattice is studied as a function of rigidity by using the Kubo–Greenwood formula. The rigidity is modulated by changing the second neighbour interactions. The results show that $\kappa(T)$ is strongly determined by the rigid character of the network through the low frequency vibrational modes. The transition from an isostatic to overconstrained lattices is thus reflected in the behavior of $\kappa(T)$.

© 2011 Elsevier B.V. All rights reserved.

1. Introduction

The physics of glass formation is a complex multiparticle problem. It depends on time, which means that basically, there is no thermal equilibrium. During glass formation the cooling speed plays an important role. If the cooling process is slow, a first order phase transition occurs resulting in a crystalline structure [1]. Therefore, in order to make a glass, it must be cooled fast enough to avoid crystallization, and there is a smooth change to a solid state at a temperature known as the glass transition temperature (T_g). The behavior of viscosity near the glass transition [1] defines the glass fragility. It can be changed from strong to fragile by chemical doping [2]. Particularly, the structure of network glasses as oxides, chalcogenides and amorphous semiconductors is similar to a network with topological disorder. It is known that most glasses have an excess of Low Frequency Vibrational Modes (LFVM) when compared with crystals. Two examples of this excess are the boson peak [3] and the floppy mode contribution. While there is not consensus about the nature of the boson peak [3,4], the floppy mode contribution can be explained very successfully by rigidity theory [5,6] considering the covalent bonding as a mechanical constrain**.** Notice that there are some indications that the Boson peak and the floppy modes share a common origin, as has been shown in a series of conclusive experiments on the binary glass [7] As_xS_{1-x}, as well as using numerical simulations [8] and perturbation techniques [9]. If the number of constraints (N_c) is lower than the degrees of freedom (dN where d is the dimension), there is a fraction $f = 1 - N_c/dN$ of zero frequency vibrational modes (floppy modes). If $f = 0$, the lattice is rigid while it is flexible for $f > 0$. When $dN = N_c$, the lattice is isostatic because it has the minimal number of constraints required to be rigid. The transition from flexible to rigid, has been documented extensively, including many interesting effects like changes in the ionic conductivity in glasses [10], fragility [2] or glass transition temperature [11–13]. Isostatic lattices have been used to investigate the elastic and vibrational properties of different systems [14–16] including network glasses [6]. Furthermore, there is evidence of a glassy phase in which atoms are organized in isostatic networks to reduce the stress [17], which is known as Boolchand's intermediate phase [18]. The anomalies in the LFVM can determine the glass transition temperature as function of chemical composition and thermal relaxation properties [19,20].

Very recently, there has been a direct measurement of the thermal conductivity as a function of rigidity for amorphous fluorocarbons [21], although there are not theoretical efforts in this direction. In fact, up to our knowledge, the only modelling of the thermal conductivity in a network glass has been made in silica [22]. In the present work, we start to investigate the thermal conductivity as a function of rigidity in network glasses. To make a clear discussion on such effects, we decided to use a simple lattice in which the rigidity can be controlled at will, in the same spirit as has been recently discussed in [8,9] or in [23]. Such model is a square lattice, in which nearest neighbor atoms are joined by springs. If periodic boundary conditions are used, the lattice is isostatic. Then we add a second neighbor interaction either at random or in a ordered way, just to increase in a progressive way the rigidity of the lattice. This model has the advantage that one can study a *rigidity transition in a periodic system*, or in a *random system*. In this work, the resulting thermal conductivities are obtained using the Kubo–Greenwood formula [24,25], and as we will see, rigidity has an impact on this conductivity as has been found experimentally. Such effect is a consequence of the changes in the number of LFVM and group velocities. The layout of this Letter is the following, in Section 2 we present the model, in Section 3 we study

* Corresponding author. Tel.: +55 56 22 51 74; fax: +55 56 22 55 08.
E-mail address: naumis@fisica.unam.mx (G.G. Naumis).

0375-9601/$ – see front matter © 2011 Elsevier B.V. All rights reserved.
doi:10.1016/j.physleta.2011.08.008

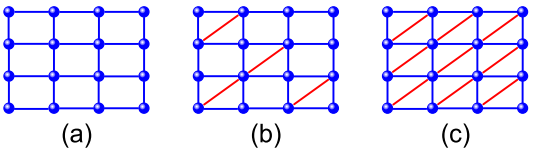

Fig. 1. (Color online.) The concentration parameter c determines the number of k_1 springs distributed along the single diagonals of a square lattice. (a) If $c = 0$, there are no k_1 springs on the lattice. (b) For $0 < c < 1$, the k_1 springs are distributed at random along the single diagonals of the lattice. (c) For $c = 1$, all single diagonals are joined by k_1 springs.

the periodic case, in Section 4 we investigate systems with different concentration of diagonal springs placed at random, and the conclusions are presented in Section 5.

2. The model

Let us consider a model which allows to understand in a transparent way the effects of rigidity. Such model is a two-dimensional square lattice made of equal masses (m) joined by springs k_0 for first neighbour interaction, using periodic boundary conditions. In order to model a network with different degrees of rigidity, we introduce a concentration parameter (c) with values between 0 and 1. This concentration determines the number of diagonals added at random to join second nearest neighbors with springs of constant k_1. When $c = 0$, there are no k_1 springs on the lattice and only first neighbour interactions are considered, as shown in Fig. 1(a). If $0 < c < 1$, besides the first neighbour interactions, the springs with constant k_1 are distributed in a random way along the single diagonals on the lattice, as shown in Fig. 1(b). For $c = 1$, there is a k_1 spring in all single diagonals, as shown in Fig. 1(c).

Clearly, there are two paths to study this system. One is to consider a lattice in which $c = 1$, resulting always in a periodic system, since all diagonals are always present. For this case, when $k_1 = 0$, the lattice is isostatic, since the coordination of the lattice is 4, and thus the number of constraints is $N_c = 2N$, which is equal to the dimensionality of the configurational space, $2N$. If $k_1 \neq 0$, the coordination of the lattice is bigger than 4. As a consequence, the number of bonds is higher than the dimension of the configurational space, and the lattice becomes rigid. The other study case is to set $k_1 \neq 0$, and move c from 0 to 1. Clearly, the limiting values $c = 0$ and $c = 1$, correspond to an isostatic and an overconstrained network respectively. Thus, in both study cases it is possible to obtain an isostatic lattice in the appropriate limits. For the periodic case, this happens when $k_1 = 0$, while for the disordered case occurs at $c = 0$. Although in this isostatic limit both periodic and disordered lattices become the same, is clear that the way in which we approach this limit is different. As a result, sometimes we will consider the limits $k_1 \to 0$ or $c \to 0$, depending on the study case.

In Section 3 we discuss the case of a rigidity transition in the periodic system, using as a control parameter k_1/k_0 to tune the rigidity, while in Section 4 we discuss the case of the random approach. Before this, let us briefly explain in the following section how the thermal conductivity is calculated.

3. Hamiltonian and thermal conductivity

To understand the thermal conductivity ($\kappa(T)$), here we consider the heat propagation along the x direction, *i.e.*, $\kappa_{xx}(T)$. The thermal conductivity can be calculated using the Kubo–Greenwood formula [24]

$$\kappa_{\alpha\beta}(T) = \frac{-2\hbar^2}{V\pi k_B T^2}\int_0^\infty d\omega \frac{\omega^2 \exp(\hbar\omega/k_B T)}{[\exp(\hbar\omega/k_B T)-1]^2} \times \mathrm{Tr}\{A^\alpha \,\mathrm{Im}[G(\omega)] A^\beta \,\mathrm{Im}[G(\omega)]\}, \tag{1}$$

where V is the system volume, T the temperature, k_B the Boltzmann constant, $\hbar$ the Planck's constant divided by 2π, $[\exp(\hbar\omega/k_B T)-1]^{-1}$ is the phonon distribution function, $A^\alpha(i,j) = \frac{1}{2}(\mathbf{r}_i - \mathbf{r}_j)_\alpha \Phi(i,j)$ the transversal or longitudinal vibrational modes, Φ is the dynamic matrix, α and β are Cartesian coordinates and $G(\omega) = (\Phi - m\omega^2 I)^{-1}$ is the Green function which can be calculated through matrix inversion [26]. The dispersion relation can be obtained by solving the secular equation for a site i in the lattice

$$\left[\sum_j^n \Phi(i,j) - m\omega^2 I\right]\mathbf{u}_i - \sum_j^n \Phi(i,j)\mathbf{u}_j = 0, \tag{2}$$

where the matrix $\Phi(i,j)$ describes the interaction between sites i and j, I is the identity matrix, $\mathbf{u}_i$ is the displacement of the mass m at site i around its equilibrium position, n is the number of neighbors joined to site i.

It is worth mentioning that Eq. (1) does not consider anharmonic interactions. Thus, our model works only for low temperatures. The concentration parameter led us to classify our systems into two study cases, the first one being a periodic lattice where $c = 0$ or $c = 1$, as shown in Figs. 1(a) and 1(c), and the second study case corresponds to networks where $0 < c < 1$, which are discussed in Section 5.

4. Thermal conductivity and rigidity for the periodic lattice

Here we present how rigidity changes the thermal conductivity by comparing results with different k_1/k_0 ratios, by fixing $c = 1$. The reason to expect important changes on the thermal conductivity is the fact that rigidity changes the number of LFVM, which are the main responsible of heat conduction due to their high group velocities.

To understand this, consider the case of an isostatic network, *i.e.*, a pure square lattice where only first neighbour interactions are included. By solving Eq. (2), it is easy to obtain the dispersion relation, which has two independent branches, corresponding to the dispersion relationship of two uncoupled linear chains

$$\omega_x(\mathbf{q}) = \frac{2v_s}{a}\left|\sin(q_x a/2)\right|, \qquad \omega_y(\mathbf{q}) = \frac{2v_s}{a}\left|\sin(q_y a/2)\right| \tag{3}$$

where a is the lattice constant, q_x and q_y are the wave vectors, v_s the speed of sound, given by $v_s = a\sqrt{k_0/m}$. The dispersion relation of Eq. (3) is shown in Figs. 2(a) and 2(b). The resulting density of states $\rho(\omega)$ is similar to that observed in a one-dimensional linear chain, and thus is a constant different from zero in the limit $\omega \to 0$, indicating a finite amount of LFVM. The isostatic network does not have transverse modes; instead two degenerate branches of longitudinal modes are present.

The rigid case, including the diagonal interaction k_1, yields the dispersion relation

$$\omega_\pm^2(\mathbf{q}) = \frac{1}{2}\left[1 \pm \eta(\mathbf{q})\right]\omega_x^2(\mathbf{q}) + \frac{1}{2}\left[1 \mp \eta(\mathbf{q})\right]\omega_y^2(\mathbf{q}) + \frac{\gamma}{2}\omega_{xy}^2(\mathbf{q}), \tag{4}$$

where γ is the ratio which controls the transition from an isostatic to an overconstrained lattice

$$\gamma = \frac{k_1}{k_0}, \tag{5}$$

with

$$\omega_{xy}^2(\mathbf{q}) = 2\frac{v_s}{a}\sin\frac{(q_x + q_y)a}{2}, \tag{6}$$

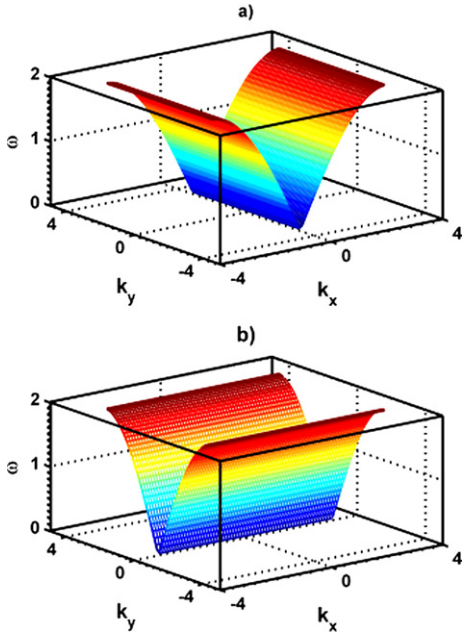

Fig. 2. (Color online.) Dispersion relation for a square lattice with only first neighbour interaction, $k_0 = 1$ and $k_1 = 0$. There are two independent degenerate branches, in (a) longitudinal modes of vibration in the x direction, and (b) longitudinal modes of vibration in the y direction.

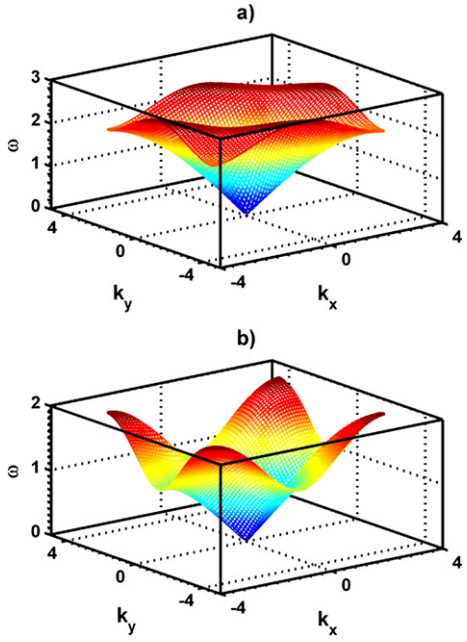

Fig. 3. (Color online.) Dispersion relation for a square lattice with $\gamma = 1$ and $c = 1$. Two branches are found in Eq. (4), (a) corresponds to the plus sign labeled as the longitudinal branch, and (b) corresponds to the minus sign labeled as the transverse branch.

and

$$\eta(\mathbf{q}) = \sqrt{1 + \gamma^2 \left[\frac{\omega_{xy}^2(\mathbf{q})}{\omega_x^2(\mathbf{q}) - \omega_y^2(\mathbf{q})} \right]^2}. \tag{7}$$

The signs in $\omega_{\pm}^2(\mathbf{q})$ are used to denote two branches, one corresponding to the longitudinal and the other to the transverse modes. The branch with plus (minus) sign is labeled as the longitudinal (transverse) branch. Both branches are depicted in Figs. 2 and 3. The case $\gamma = 0$ is shown in Fig. 2, and shows how Eq. (4) is reduced to $\omega_x(\mathbf{q})$ and $\omega_x(\mathbf{q})$, corresponding to one-dimensional lattices. Fig. 3 corresponds to a ratio of spring constants $\gamma = 1$, showing the two branches. In the acoustic limit, the dispersion relation has the following form,

$$\omega_{\pm}(\mathbf{q}) \approx \frac{v_s}{\sqrt{2}} f_{\pm}(\theta) q, \tag{8}$$

where $f_{\pm}(\theta)$ is the direction dependence of the speed of sound for longitudinal (plus sign) and transverse (minus sign) modes

$$f_{\pm}^2(\theta) = \left[1 + \gamma(1 + \sin 2\theta) \pm \sqrt{\cos^2 2\theta + \gamma^2 (1 + \sin 2\theta)^2} \right]. \tag{9}$$

For $\gamma = 1$, the resulting $\rho(\omega)$ in the acoustic region goes as $\rho(\omega) \sim \omega$, and $\rho(\omega) \to 0$ as $\omega \to 0$, as expected for a rigid system. When $\gamma = 0$, $v_+^2(\theta) = v_-^2(\theta)$ and we recover Eq. (3), with a finite $\rho(\omega)$ at $\omega \to 0$. As a consequence, a rigidity transition occurs when $\gamma \to 0$. Fig. 4 shows the Density Of States (DOS) for both systems. The gray line corresponds to $\gamma = 0$ and the black to $\gamma = 1$, confirming the results shown in Figs. 2 and 3. In this way, many LFVM are eliminated when $k_1 \neq 0$. These states are the main heat carriers and one can expect changes in the thermal conductivity, as we will see next.

Once that the rigidity transition has been established, we turn our attention towards the thermal conductivity $\kappa_{xx}(T)$. To calculate $\kappa_{xx}(T)$, we used a square lattice with 50 sites along each spatial direction x and y. At this point, it is worthwhile mentioning that throughout the whole Letter, we have performed all calculations in lattices of sizes of 15×15, 20×20 and sometimes of 30×30 sites. In all cases, we will show the obtained data for systems of 50×50 sites, since we are using periodic boundary conditions, and the size effects are not so important as the results show a good convergence. The convergence is weaker as the isostatic limit is approached, basically because the lattices become closer to a set of independent linear chains. Thus, a lattice of 50×50 sites behaves as a degenerate system of 50 chains of 50 sites, which is certainly small for a linear system. In these cases, we considered bigger chains to verify the validity of our results. However, in this limit we have the analytical solution for the problem, and thus the scaling effects are easy to understand.

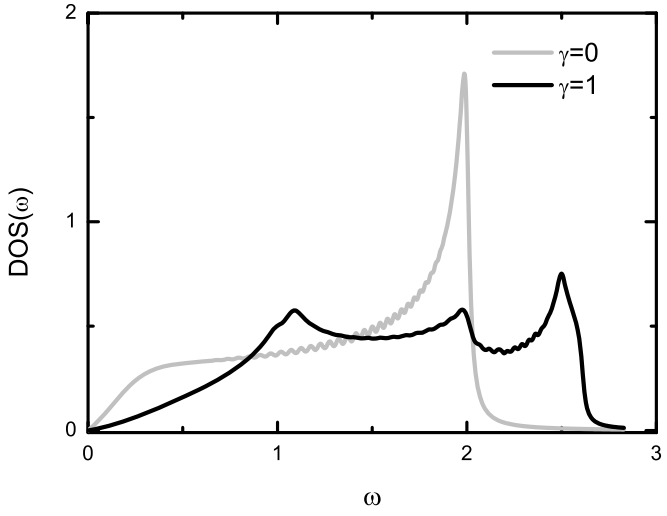

Fig. 4. Density of states for a square lattice with only first neighbour interaction $\gamma = 0$ (grey line), and second neighbour interaction $\gamma = 1$ (black line), both are periodic systems with $c = 1$. Notice how the number of LFVM changes with γ.

The Green function was obtained through matrix inversion and by using Eq. (1). The inset in Fig. 5 shows $\kappa_{xx}(T)$ in the low temperature region for different values of the γ ratio. The black,

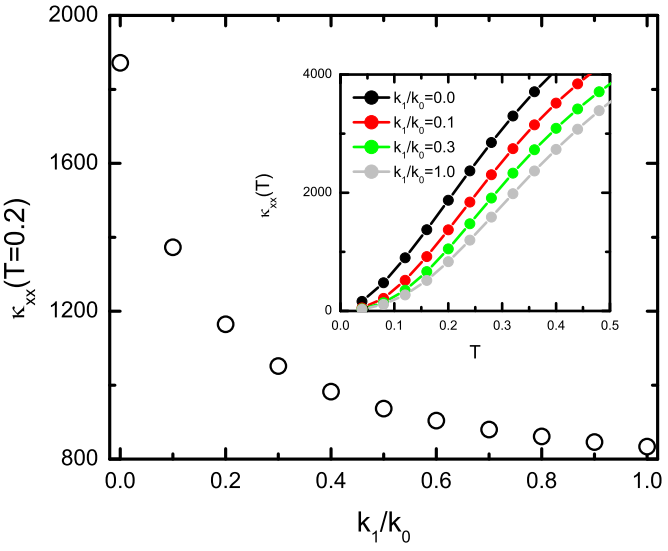

Fig. 5. (Color online.) Thermal conductivity states for a square lattice of 2500 sites with $c = 1$ at a low temperature, $T = 0.2$. Each lattice has 50×50 sites. In the inset, we show $\kappa_{xx}(T)$ for different $\gamma = k_1/k_0$ ratios. $\gamma = 0.1$ (red circles), $\gamma = 0.3$ (green circles) and $\gamma = 1.0$ (gray circles) ratios. The thermal conductivity systematically diminishes as function of the γ ratio. The highest $\kappa_{xx}(T)$ is obtained for a concentration $\gamma = 0$.

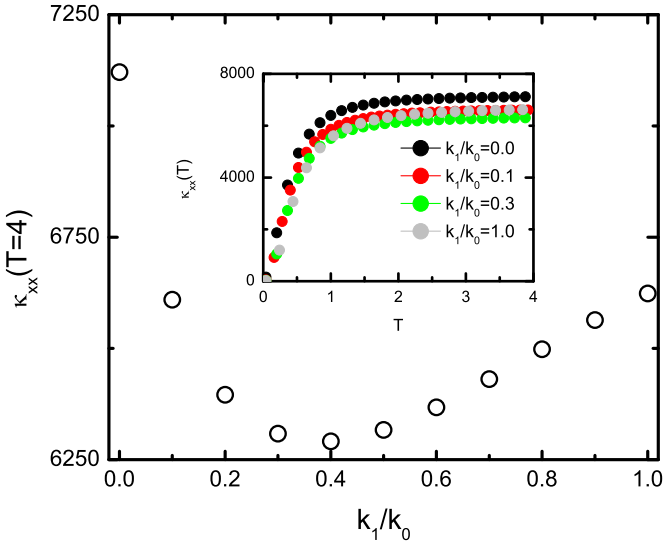

Fig. 6. (Color online.) Thermal conductivity for periodic square lattices at a high temperature, $T = 4.0$. Each lattice has 50×50 sites When the ratio γ is in the range $0 < \gamma < 0.4$, the thermal conductivity falls because there are less LFVM. For $0.4 < \gamma < 1.0$, the phonon group velocity is increased, which in turn increases the thermal conductivity as well. It is worth mentioning that anharmonic interactions are not considered in this model. In the inset, we present the behavior of $\kappa_{xx}(T)$ in a wide range of temperatures for $\gamma = 0$ (black circles), $\gamma = 0.1$ (red circles), $\gamma = 0.3$ (green circles) and $\gamma = 1.0$ (gray circles). Again, the highest $\kappa_{xx}(T)$ is found for the system with $\gamma = 0$.

red, green and gray lines correspond to $\gamma = 0.0, 0.1,\ 0.3$ and 1.0 respectively. Notice that the lower thermal conductivity corresponds to the $\gamma = 1$ ratio, while the best thermal conductivity is obtained for the $\gamma = 0$ ratio. When $\gamma \to 0$, $\kappa_{xx}(T)$ grows systematically for fixed T. To see this, Fig. 5 shows the typical behavior of $\kappa_{xx}(T)$ for a given temperature (in this case $T = 0.2$) as a function of the γ ratio. A diminishing $\kappa_{xx}(T)$ can be observed with γ.

An analysis of the high temperature regimen is shown in Fig. 6. Notice that in real systems, such limit cannot be obtained from the sole use of the harmonic Hamiltonian, since non-linear effects appear. However, for the sake of completeness, here we present the corresponding results. The inset in Fig. 6 shows the same curves as in Fig. 5, for a wider range of temperatures. Notice how $\kappa_{xx}(T)$ diminishes immediately as the ratio γ becomes different from 0, as shown by the red curve ($\gamma = 0.1$) and the green curve ($\gamma = 0.3$). The behavior of $\kappa_{xx}(T)$ is clear in Fig. 6, where the plot shows $\kappa_{xx}(T)$ for a given high temperature $T = 4$, versus the γ ratio. The lowest thermal conductivity seems to be for the ratio value $\gamma = 0.4$, then $\kappa_{xx}(T)$ starts to grow as shown in Fig. 6, and by the gray curves ($\gamma = 1$) in the inset of Fig. 6.

Let us now explain in detail why a rigidity transition has an expected effect on the thermal conductivity. Within the framework of the kinetic theory of gases, the thermal conductivity can be written as an integral in the reciprocal $\mathbf{q}$-space [27]

$$\kappa_{xx}(T) = \int_{1st\,BZ} d\boldsymbol{q}\, \tau_{\mathbf{q}} v_{q_x}^2 C_{\mathbf{q}}, \tag{10}$$

where $C_{\mathbf{q}}$ is the heat capacity, $v_{q_x} = \partial\omega(\mathbf{q})/\partial q_x$ is the x component of the phonon group velocity, and $\tau_{\mathbf{q}}$ is the relaxation time. In our case, we do not consider phonon scattering, so $\tau_{\mathbf{q}}$ is a constant mean free path τ in all cases. Using the Bose–Einstein statistics, $C_{\mathbf{q}}$ is given by

$$C_{\mathbf{q}} = \frac{d}{dT}\left[\frac{\hbar\omega(\mathbf{q})}{e^{\hbar\omega(\mathbf{q})/k_BT} - 1}\right]. \tag{11}$$

Since LFVM have the highest group velocities, we can consider that $\omega_{\pm}(\mathbf{q}) \approx v_{\pm}(\theta)q$ and $v_{q_x} = \nabla_{\mathbf{q}}\omega_{\pm}(\mathbf{q}) \cdot \hat{e}_x$. It follows that

$$\begin{aligned}\kappa_{xx}(T) &\approx \frac{4\tau}{\Omega}\frac{\hbar^2 v_s^4}{k_B T^2} \\ &\times \sum_{\pm}\left[\int_0^{\pi/4}\int_0^{\frac{\pi}{a\cos\theta}} + \int_{\pi/4}^{\pi/2}\int_0^{\frac{\pi}{a\sin\theta}}\right]\frac{[f_{\pm}(\theta)\cos\theta - f'_{\pm}(\theta)\sin\theta]^2}{(e^{\hbar v_s f_{\pm}(\theta)q/\sqrt{2}k_BT} - 1)^2} \\ &\times e^{\hbar v_s f_{\pm}(\theta)q/\sqrt{2}k_BT} f_{\pm}^2(\theta) q^3\, dq\, d\theta,\end{aligned} \tag{12}$$

where the sum is carried over the longitudinal and transversal mode branches, and Ω is a proper normalization for the number of states for an unitary area $\Omega = (2\pi)^2$. Usually, for low temperatures, the Bose–Einstein factor can be replaced by a decreasing exponential, which has a maximum for LFVM. This explains the importance of such modes for low temperatures. Furthermore, this allows to obtain the Debye law in which $C_{\mathbf{q}} \propto (\Theta/T)^d$ where Θ is the Debye temperature. Although this is correct for $\gamma \approx 1$, the usual procedure of letting $T \to 0$ and transform the integrals using infinite as a boundary condition, cannot be used in such a simple way in Eq. (12) when $\gamma \to 0$, since Θ depends on the angle θ. So for example, Θ can be nearly zero in a certain directions. Such behavior leads to the required changes of $C_{\mathbf{q}}$ with the dimensionality as $\gamma \to 0$. In particular, Eq. (12) can be written as

$$\kappa_{xx}(T) \approx \alpha(\gamma)T^2 + \beta(\gamma)T, \tag{13}$$

where $a(\gamma)$ and $b(\gamma)$ are given in Appendix A. Two very important limiting cases are easily worked out. For $\gamma = 0$, and a system of $N \times N$, the conductivity corresponds to a one-dimensional system

$$\kappa_{xx}(T) \approx \frac{Nk_B^2}{2\pi\hbar}T \tag{14}$$

while for $\gamma = 1$

$$\kappa_{xx}(T) \approx \frac{3Nak_B^3}{2\pi^2 v_s \hbar^2}T^2. \tag{15}$$

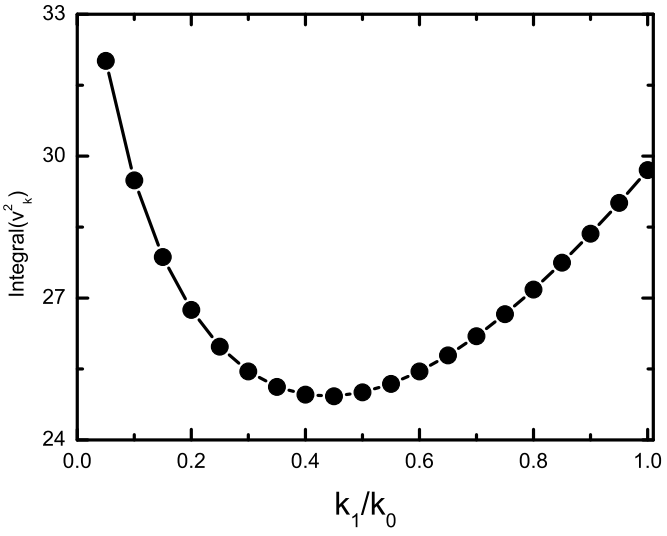

Fig. 7. Square group velocity integrated in the first Brillouin zone for square lattices with $c = 1$ as function of the γ ratio, obtained from the dispersion relation of Eq. (4). The behavior is the same as the high temperature thermal conductivity in Fig. 6.

This result is fully two-dimensional, showing that the rigidity transition basically produces a change in the dimensionality of the problem, since for periodic systems $\kappa_{xx}(T) \propto T^d$.

For real systems in the high temperature regime, anharmonic effects are important. However, in our case it can serve as an additional test for the simulations. Therefore, in this limit, each mode contribute with

$$C_{\mathbf{q}} = \frac{k_B}{2} \tag{16}$$

and $\kappa_{xx}(T)$ is

$$\kappa_{xx}(T) = \frac{k_B \tau}{2} \int_{1st\ BZ} d\boldsymbol{q}\, v_{q_x}^2. \tag{17}$$

An analytical result for previous integral can be readily obtained from Eqs. (3) and (4). It can also be obtained through numerical differentiation from the dispersion relation, as the one shown in Figs. 2 and 3 for the different γ ratios. Fig. 7 shows that the behavior of v_k^2 is similar to that for $\kappa_{xx}(T)$ in the high temperature region, when compared with Fig. 6, as expected.

The behavior of the thermal conductivity for network glasses modeled by square lattices with different values of concentration is discussed in the next section.

5. Lattices with different concentration

In this section, we discuss the behavior of $\kappa_{xx}(T)$ as a function of the concentration (c). Fig. 8 shows $\kappa_{xx}(T)$ for various concentrations of diagonals, $c = 1.0$ (black circles), $c = 0.8$ (green circles) and $c = 0.2$ (red circles) for different γ ratios, in (a) $\gamma = 1$, (b) $\gamma = 0.5$ and (c) $\gamma = 0.1$. In all of these plots, we include an inset presenting an amplification of the low temperature region. All computations were made for lattices of 50×50 sites.

First we observe that in Fig. 8(a), corresponding to $\gamma = 1$, the behavior is determined by c. At high temperatures, $\kappa_{xx}(T)$ has a minimum saturation value as a function of c. So for example, the cases $c = 0.2$ and $c = 0.8$ have almost the same $\kappa_{xx}(T)$. The cases $c = 1.0$ and $c = 0.0$ are just the limiting cases that

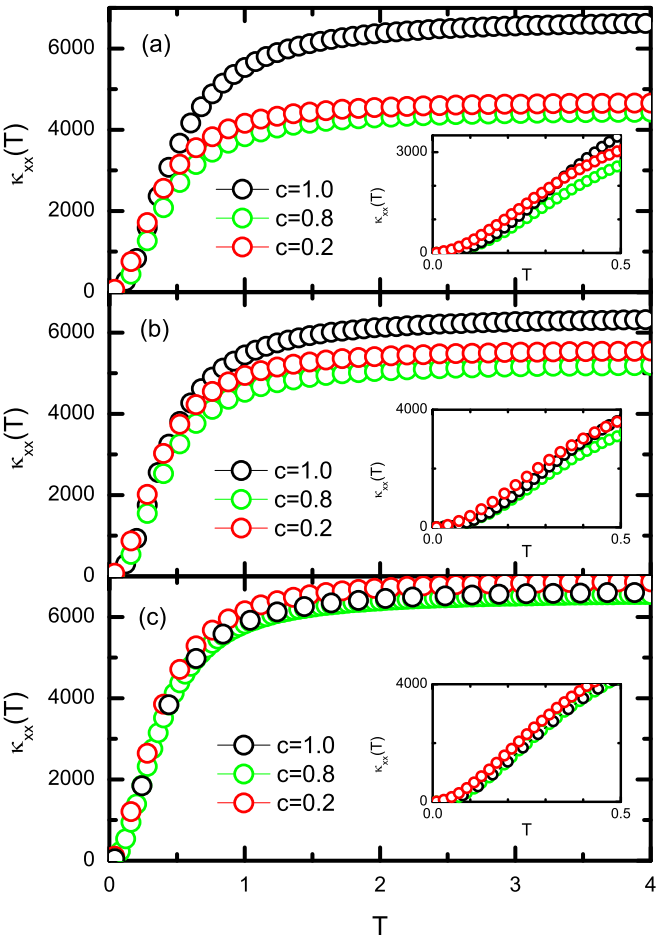

Fig. 8. (Color online.) The behavior of $\kappa_{xx}(T)$ for square lattices with different concentrations c of diagonals placed at random, for different $\gamma = k_1/k_0$ ratios. (a) $k_1/k_0 = 1$, (b) $k_1/k_0 = 0.5$ and (c) $k_1/k_0 = 0.1$. The insets are amplifications of the low temperature region.

coincide with the periodic lattices, for which we know that for $c = 1.0$, $\kappa_{xx}(T)$ is a little bit smaller than for the $c = 0.0$ case (see Fig. 6). For low temperatures, as seen in the inset of Fig. 8(a), the behavior is reversed. In Fig. 8(b) there is a mixing of c and γ effects, but the overall behavior is similar to that observed in Fig. 8(a), although the values of $\kappa_{xx}(T)$ come closer to each other. Finally in Fig. 8(c), the effects of the concentration are minimal, since γ is small so the results are similar to those of the isostatic network, as expected. We can understand these trends as follows. The general effect of the concentration is to modify the number of constraints, group velocities and localization properties for high frequency modes, above the mobility edge known as Ishii limit [20]. Therefore, when c is small there are more LFVM and $\kappa_{xx}(T)$ can grow if these effects are more important than the changes in the group velocities, since localization effects are not so important for acoustic modes. This effect can be observed in the inset of each figure, where the thermal conductivity is shown for the low temperature region. The case $c = 0.2$ (red circles) has the best thermal conductivity and the range where $\kappa_{xx}(T)$ is higher is a function of γ. Particularly, when c and γ are both small, the thermal conductivity is higher than for the periodic case with $c = 1$ along the whole range of temperatures, as shown in Fig. 8(c). In the high temperature limit, the balance is subtle. All modes contribute the same, and $\kappa_{xx}(T)$ depends on localization and group velocities. Maximal disorder occurs for $c = 0.5$, while the group velocities depend on the Ishii limit [20].

6. Conclusions

In this Letter, the effects of rigidity in the thermal conductivity were studied by means of the Kubo–Greenwood formula. The rigidity is determined by two parameters, the springs constant $\gamma = k_1/k_0$ ratio, and the concentration c of second neighbour springs. Both parameters modify the number of LFVM and the phonon group velocity. For periodic lattices, the results are the following.

1) At low T, the behavior is dominated by the heat capacity. The reason is that only LFVM are excited. Rigidity plays a fundamental role since it determines the specific heat through the number of LFVM. As a result, $\kappa_{xx}(T) \sim T$ for the isostatic lattice, while $\kappa_{xx}(T) \sim T^2$ for overconstrained networks.

2) At high T, all modes are excited with the same energy, so the conductivity is dominated by the integral of the group velocity in the first Brillouin zone. We obtained that there is a minimum for such integral at $\gamma \approx 0.4$, which coincides with the minimum obtained from $\kappa_{xx}(T)$ using the Kubo–Greenwood formula. However, here we do not consider non-linear effects which are fundamental in such regimen.

The reason for this change comes from the fact that here, the isostatic lattice is equivalent to a set of linear chains, since there is no coupling between displacements in perpendicular directions. Then we recover case of a linear chain in which $\kappa_{xx}(T) \sim T$. When the such couplings are turned on, the chains interact between them and thus the system behaves as a two-dimensional system in which $\kappa_{xx}(T) \sim T^2$.

For disordered lattices, the situation is more complex.

1) At low T, for a given γ ratio, there is a crossover of $\kappa_{xx}(T)$ as a function of the concentration of disorder. In general, again isostatic lattices have a larger $\kappa_{xx}(T)$ than overconstrained. This is a consequence of the fact that acoustic modes have mainly the same localization properties, even in the presence of disorder [20]. The excess of LFVM for isostatic lattices determines this better thermal conductivity, as in periodic lattices.

2) At high T, the heat capacity does not play a role. Here the group velocities and the Ishii limit are the main driving factors [20] which determine $\kappa_{xx}(T)$. However, since here we do not consider non-linear effects, the calculation of $\kappa_{xx}(T)$ is only a first step towards the complete answer.

Finally, although it could be worth to show some comparison with experimental data of flexible and rigid systems, still there are not available systematic experimental data of $\kappa_{xx}(T)$ considering average coordination and temperature. There are some experiments for the average coordination and the minimal $\kappa_{xx}(T)$, which seem to be in good agreement with the idea of deplete bonds on rigid lattices [21].

Acknowledgements

We thank DGAPA-UNAM project IN-100310-3. F. Salazar thanks CONACYT and Posgrado de Ciencias Físicas, UNAM for a posdoctoral scholarship. All calculations were performed at Kanbalam and Bakliz supercomputers at DGSCA-UNAM.

Appendix A

Starting from Eq. (4), if $\gamma \neq 0$, then $f_\pm(\theta)$ is only zero at the origin. Then we can replace the Bose–Einstein factor with a pure exponential for low enough temperatures. Thus, Eq. (12) can be written as

$$\kappa_{xx}(T) \approx \frac{\tau}{\Omega}\frac{\hbar^2 v_s^4}{k_B T^2}\sum_{\pm}\left[\int_0^{\pi/4}\int_0^{\frac{\pi}{a\cos\theta}} + \int_{\pi/4}^{\pi/2}\int_0^{\frac{\pi}{a\sin\theta}}\right] R_\pm(\theta) \times f_\pm^4(\theta) e^{-c_\pm q} q^3\, dq\, d\theta, \tag{A.1}$$

where

$$R_\pm(\theta) = \left[\cos\theta - \frac{f'_\pm(\theta)}{f_\pm(\theta)}\sin\theta\right]^2, \tag{A.2}$$

and

$$c_\pm = \frac{\hbar v_s f_\pm(\theta)}{\sqrt{2}k_B T}. \tag{A.3}$$

Then we integrate over the q coordinate to get

$$\kappa_{xx}(T) \approx \frac{\tau}{\Omega}\frac{k_B^3}{\hbar^2}T^2\sum_{\pm}\left[\int_0^{\pi/2} R_\pm(\theta)\, d\theta - \int_0^{\pi/4} R_\pm(\theta) H_1(\theta, T)\, d\theta - \int_{\pi/4}^{\pi/2} R_\pm(\theta) H_2(\theta, T)\, d\theta\right] \tag{A.4}$$

where the functions $H_n(\theta, T)$ are defined as

$$H_n(\theta, T) \equiv e^{-c_\pm x_n(\theta)}\left\{6 + 6c_\pm x_n(\theta) + 3c_\pm^2 x_n^2(\theta) + c_\pm^3 x_n^3(\theta)\right\} \tag{A.5}$$

with

$$x_1(\theta) = \frac{\pi}{a\cos\theta}, \qquad x_2(\theta) = \frac{\pi}{a\sin\theta}. \tag{A.6}$$

Notice that in Eq. (A.4), the leading contribution is the conductivity of a two-dimensional lattice, with an angle averaged group velocity. The correction terms have an exponential which in principle goes to zero as $T \to 0$. Such condition is equivalent to

$$c_\pm x_n(\theta) = \frac{\hbar v_s f_\pm(\theta)}{\sqrt{2}k_B T} x_n(\theta) \gg 1. \tag{A.7}$$

However, when $\gamma \ll 1$, in certain directions the opposite behavior turns out to be true

$$c_\pm x_n(\theta) \ll 1$$

since $f_\pm(\theta)$ can be nearly zero. We can incorporate both behaviors in Eq. (A.5) as follows. For $c_\pm x_n(\theta) \gg 1$, the exponential term is zero, while for $c_\pm x_n(\theta) \ll 1$, we can use an angle θ_M such that $f_\pm(\theta_M)$ is a minimum, and expand $f_\pm(\theta)$ in a Taylor series

$$f_\pm(\theta) \approx f_\pm(\theta_M) + \left|f''_\pm(\theta_M)\right|\frac{(\theta - \theta_M)^2}{2}. \tag{A.8}$$

For this case, in Eq. (A.5) we only retain the zero and first order terms in $c_\pm x_n(\theta_M)$ and the exponential factor is nearly one. As a result, $\kappa_{xx}(T)$ can be written as

$$\kappa_{xx}(T) \approx \alpha(\gamma)T^2 + \beta(\gamma)T, \tag{A.9}$$

where $a(\gamma)$ and $\beta(\gamma)$ are given by

$$a(\gamma) \approx \frac{6N}{\pi^2}\frac{a k_B^3}{v_s \hbar^2}\sum_{\pm}\left[\int_0^{\pi/2} R_\pm(\theta) \times \left\{1 - e^{-\frac{\hbar v_s}{\sqrt{2}k_B T}\left|f''_\pm(\theta_M)\right|\frac{(\theta-\theta_M)^2}{2}}\right\} d\theta\right], \tag{A.10}$$

and

$$\beta(\gamma) \approx -\frac{6N}{\sqrt{2}\pi}\frac{k_B^2}{\hbar}\sum_{\pm}\left\{\int_0^{\pi/4}\frac{R_{\pm}(\theta)}{\cos\theta}\left[f_{\pm}(\theta_M) + \left|f''_{\pm}(\theta_M)\right|\frac{(\theta-\theta_M)^2}{2}\right]d\theta + \int_{\pi/4}^{\pi/2}\frac{R_{\pm}(\theta)}{\sin\theta}\left[f_{\pm}(\theta_M) + \left|f''_{\pm}(\theta_M)\right|\frac{(\theta-\theta_M)^2}{2}\right]d\theta\right\}. \tag{A.11}$$

In the previous approximation, it was used that $\tau \approx Na/v_s$. Notice that in principle, if in Eq. (A.5) we use the term that goes as $(c_{\pm}x_n(\theta))^3$, there is a $1/T$ divergence. In fact, such divergence is an artifact due to the approximation, *i.e.*, if such term is enough important to be considered, then $e^{-c_{\pm}x_n(\theta)}$ is small enough to kill the divergence.

References

[1] P.G. Debenedetti, F.H. Stillinger, Nature 410 (2000) 259.
[2] M. Tatsumisago, B.L. Halfpap, J.L. Green, S.M. Lindsay, C.A. Angell, Phys. Rev. Lett. 64 (1990) 1549.
[3] K. Binder, W. Kob, Glassy Materials and Disordered Solids, first ed., World Scientific, Singapore, 2005.
[4] G. D'Angelo, G. Carini, C. Crupi, M. Koza, G. Tripodo, C. Vasi, Phys. Rev. B 79 (2009) 014206.
[5] J.C. Phillips, J. Non-Cryst. Solids 34 (1979) 153.
[6] M.F. Thorpe, J. Non-Cryst. Solids 57 (1983) 355.
[7] Ping Chen, Chad Holbrook, P. Boolchand, D.G. Georgiev, K.A. Jackson, M. Micoulaut, Phys. Rev. B 78 (2008) 224208.
[8] H.M. Flores-Ruiz, G.G. Naumis, J.C. Phillips, Phys. Rev. B 82 (2010) 214201.
[9] H.M. Flores-Ruiz, G.G. Naumis, Phys. Rev. B 83 (2011) 184204.
[10] D.I. Novita, P. Boolchand, M. Malki, M. Micoulaut, Phys. Rev. Lett. 98 (2007) 195501.
[11] G.G. Naumis, R. Kerner, J. Non-Cryst. Solids 231 (1998) 111.
[12] G.G. Naumis, J. Non-Cryst. Solids 352 (2006) 4865.
[13] G.G. Naumis, Phys. Rev. B 73 (2006) 172202.
[14] D.J. Jacobs, M.F. Thorpe, Phys. Rev. Lett. 75 (1995) 4051.
[15] A.V. Tkachenko, T.A. Witten, Phys. Rev. E 60 (1999) 687.
[16] C. Heussinger, B. Schaefer, E. Frey, Phys. Rev. E 76 (2007) 031906.
[17] D. Selvanathan, W.J. Bresser, P. Boolchand, Phys. Rev. B 61 (2000) 15061.
[18] M. Micoulaut, M. Malki, Phys. Rev. Lett. 105 (2010) 235504.
[19] J.R. Romero-Arias, G.G. Naumis, Phys. Rev. E 77 (2008) 061504.
[20] J.R. Romero-Arias, F. Salazar-Posadas, G.G. Naumis, Phil. Trans. R. Soc. A 367 (2009) 3173.
[21] M.G. Ghossoub, Lee Jung-Hyun, O.T. Baris, D.G. Cahill, S. Sinha, Phys. Rev. B 82 (2010) 195441.
[22] P. Jund, R. Jullien, Phys. Rev. B 59 (1991) 13707.
[23] A. Souslov, A.J. Liu, T.C. Lubensky, Phys. Rev. Lett. 103 (2009) 205503.
[24] R.J. Elliot, J.A. Krumhansl, P.L. Leath, Rev. Mod. Phys. 46 (1974) 465.
[25] J.K. Flicker, P.L. Leath, Phys. Rev. B 6 (1973) 2296.
[26] E.N. Economou, Green's Functions in Quantum Physics, third ed., Springer Series in Solid State Sciences, Springer, New York, 1983.
[27] S. Lepri, R. Livi, A. Politi, Phys. Rep. 377 (2003) 1.